Appl. Phys. B 75, 649–654 (2002)
DOI: 10.1007/s00340-002-1021-6

Applied Physics B
Lasers and Optics

K. OSVAY[1,✉]
P. DOMBI[1,2]
A.P. KOVÁCS[1]
Z. BOR[1,3]

Fine tuning of the higher-order dispersion of a prismatic pulse compressor

[1] Department of Optics and Quantum Electronics, University of Szeged, P.O. Box 406, Szeged 6701, Hungary
[2] Institut für Photonik, Technische Universität Wien, Gusshausstr. 27, 1040 Wien, Austria
[3] HAS Research Group on Laser Physics, University of Szeged, Dóm tér 9, Szeged 6720, Hungary

Received: 16 April 2002
Published online: 15 November 2002 •

ABSTRACT The wavelength-dependent thermal refractive index gives an extra degree of freedom for adjustment of higher-order dispersion of a prismatic pulse compressor. The effect allows of fine tuning of both intracavity and extracavity dispersion of ultra-fast oscillators. The calculations have been carried out using a new and rather handy formalism, which describes the operation of a prism pulse compressor as a linear function of the ratio of the total glass path in the prisms and the prism apex distance. The validity of theoretical calculations is supported by experimental evidence.

PACS 42.65.Re; 42.60.Da; 42.65.Ky; 42.62.Eh

1 Introduction

At the moment of the first successful generation of a sub-10-fs laser pulse [1], it became evident that in order to obtain transform-limited femtosecond pulses the resultant dispersion of the system has to be compensated not only to the second order, that is for the group-delay dispersion (GDD), but at least to the third-order dispersion (TOD). The recent revolution of the generation of femtosecond pulses by Kerr-lens mode locking (KLM) [2] made it possible for sub-50-fs laser oscillators to become an everyday tool in many research laboratories in the fields of physics, biology and chemistry. The dispersion of these lasers was first compensated by a prism pair made of optical material of proper choice [3] or a Proctor–Wise prism sequence exhibiting lower TOD [4, 5] and later by chirped mirrors [6]. To construct an oscillator producing sub-10-fs pulses with > 5-nJ energy, a long Ti:sapphire crystal should be used. In this case, however, the increased intracavity dispersion compensation can be achieved most generally by the use of appropriately designed chirped mirrors in combination with an intracavity prism compressor [7–12]. However, due to the inherent nature of these ultra-fast mirrors, i.e. the GDD and TOD curves are higher-order polynomial functions of frequency [13, 14], and also to inaccuracy in the production of these complicated dielectric layers, there is always some residual TOD (and higher-order dispersion components) in the cavity, which sets an ultimate limit for the generation of the shortest possible pulses [15, 16].

The pulses coming from the oscillator pass usually more dispersive elements, besides the thick end mirror of the cavity, like beam splitters, an object plate, a cuvette wall, etc., and are much lengthened before hitting the target. Consequently, the extracavity dispersion to be precisely compensated changes experiment by experiment. In most cases the well-known methods of fine external dispersion compensation cannot be counted on. The external chirped mirrors are not flexible enough; that is once the mirrors are produced there is no possibility of even slight adjustment of their dispersion properties. A more serious pulse shaper, based on an expensive grating pair along with a liquid-crystal modulator [17], deformable mirror [18], acousto-optical modulator [19] or thermal slab [20], cannot be afforded not only because of the costs but also the losses in those systems.

For short UV pulses, the problem of fine pre-target dispersion compensation is even more serious [21], due to higher dispersion of optical materials and also to the lack of available chirped mirrors. The recently available femtosecond, soft-UV pulses [22–26] certainly call for a device by which the dispersion can be compensated at least to the third order.

In this paper we propose a new method for the fine tuning of intracavity and extracavity dispersion. In order to suggest a solution for both problems we first reconsider the theory of prismatic pulse compressors. It is shown that all the important parameters of a prismatic compressor scale with the ratio of the total glass path and the prism apex distance. The only remaining independent parameter is the temperature of the prism material. We shall prove that the change of the material temperature of a prism pair results in a change of the ratio of GDD and TOD.

2 A generalised description of a prism-pair compressor

It is widely known that the GDD of a prism pair, that is the second derivative of phase shift $\phi(\omega)$ with respect to ω, can be adjusted simply by changing the position of either of the prisms [27–29]. It is also an inherent feature of such prism pairs that the TOD changes at the same time. Martinez et al.'s elegant model of 'crossed parallel slabs' [27] gave the

✉ Fax: +36-62/544658, E-mail: osvay@physx.u-szeged.hu

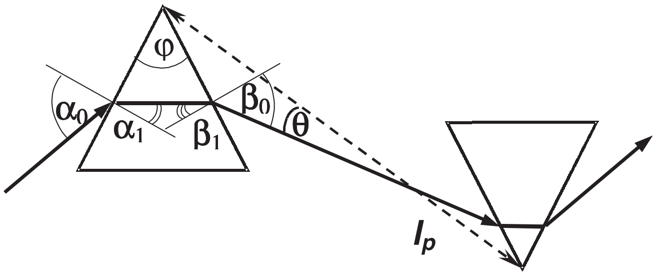

FIGURE 1 The geometry of a prismatic pulse compressor assuming the refractive faces parallel to each other

first analytical description of phase shift by a prism pair as

$$\phi(\omega) = \frac{\omega}{c} l_{\mathrm{p}} \cos\theta(\omega), \tag{1}$$

where l_{p} is the prism apex distance and c is the velocity of light in the medium between the prisms (Fig. 1). In the following we assume c to be equal to the light velocity in vacuum. The scientific community had been in doubt over (1) mainly because it seemed not to have taken into account the unavoidable propagation of light in the prism materials (see e.g. [30]), which results in positive group-delay dispersion [31]. Recently, Sherriff [32] has shown that the results obtained by using complicated ray tracing are identical to that of calculated from (1). Throughout this paper we neglect any disturbing effects such as non-parallel refracting surfaces and beam deviations [33].

2.1 *Specific dispersions*

In everyday laboratory practice, it is hard to measure the angle $\theta(\omega)$ with the necessary precision. Tuning the prism compressor, moreover, often means the change of the glass path in either of the prisms. The total glass path l_{g}, that is the sum of the geometrical light paths of both prisms can be, however, more easily determined. After some algebra, using the notation of Fig. 1, one can obtain

$$l_{\mathrm{g}} = l_{\mathrm{p}} \frac{\sin\theta \sin\varphi}{\cos\alpha_1 \cos\beta_0}, \tag{2}$$

where the wavelength-dependent α_1, β_0 angles can be calculated from the angle of incidence at the first prism α_0, the prism apex angle φ and the refractive index n as

$$\alpha_1 = \arcsin\left(\frac{\sin\alpha_0}{n}\right), \qquad \beta_0 = \arcsin\left(n \sin(\varphi - \alpha_1)\right) . \tag{3}$$

Now introducing the specific phase shift ϕ_{S} as the phase shift per unit prism apex distance, (1) can be re-written as

$$\phi_{\mathrm{S}} = \frac{\phi}{l_{\mathrm{p}}} = \frac{\omega}{c} \sqrt{1 - \left(R \frac{\cos\alpha_1 \cos\beta_0}{\sin\varphi}\right)^2}, \tag{4}$$

where R is the ratio of the total glass path to the prism apex distance ($R = l_{\mathrm{g}}/l_{\mathrm{p}}$). The specific group-delay dispersion ($\mathrm{GDD_S}$) and the specific third-order dispersion ($\mathrm{TOD_S}$), defined similarly to ϕ_{S}, are

$$\mathrm{GDD_S} = \frac{\partial^2 \phi_{\mathrm{S}}}{\partial\omega^2} = \frac{1}{l_{\mathrm{p}}} \frac{\partial^2\phi}{\partial\omega^2} \text{ and } \mathrm{TOD_S} = \frac{\partial^3 \phi_{\mathrm{S}}}{\partial\omega^3} = \frac{1}{l_{\mathrm{p}}} \frac{\partial^3\phi}{\partial\omega^3}, \tag{5}$$

respectively. Since in the everyday practice the dispersion of optical components is usually described in wavelength rather than frequency, the specific dispersion of (5) can be expressed as

$$\mathrm{GDD_S} = \left(\frac{\lambda^2}{2\pi c}\right)^2 \left(\frac{2\pi}{\lambda} \frac{\cos\alpha_1 \cos\beta_0}{\sin\varphi} \frac{\mathrm{d}^2\beta_0}{\mathrm{d}\lambda^2} R - \left(\frac{\mathrm{d}\beta_0}{\mathrm{d}\lambda}\right)^2 \phi_{\mathrm{S}}\right) \tag{6}$$

and

$$\begin{aligned} \mathrm{TOD_S} = \frac{-\lambda^5}{(2\pi c)^3} \Bigg[& \frac{2\pi}{\lambda} \frac{\cos\alpha_1 \cos\beta_0}{\sin\varphi} \\ & \times \left(\lambda \frac{\mathrm{d}^3\beta_0}{\mathrm{d}\lambda^3} + 3 \frac{\mathrm{d}^2\beta_0}{\mathrm{d}\lambda^2} - \lambda \left(\frac{\mathrm{d}\beta_0}{\mathrm{d}\lambda}\right)^3\right) \\ & \times R - 3 \frac{\mathrm{d}\beta_0}{\mathrm{d}\lambda} \left(\frac{\mathrm{d}\beta_0}{\mathrm{d}\lambda} + \lambda \frac{\mathrm{d}^2\beta_0}{\mathrm{d}\lambda^2}\right) \phi_{\mathrm{S}} \Bigg] . \end{aligned} \tag{7}$$

The first part of both $\mathrm{GDD_S}$ and $\mathrm{TOD_S}$, which is linear in R, dominates the values of the specific dispersion. Noticeable deviation from linearity in R can be expected only for highly dispersive materials, like SF10, and in the practically seldom-used region of $R > 100\%$ (Fig. 2a). A typical prism compressor such as, for instance, fused-silica prisms at Brewster angle operating at 800 nm, can then be described as follows. Starting R from zero, where the light of the centre wavelength

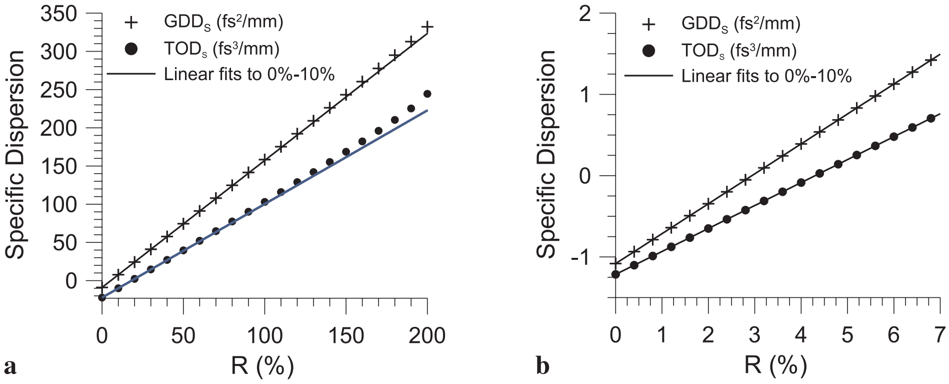

FIGURE 2 Specific group-delay dispersion ($\mathrm{GDD_S}$) and specific third-order dispersion ($\mathrm{TOD_S}$) at 800 nm for a single-pass Brewster-angle prism compressor made of SF10 (**a**) and fused silica (**b**)

is assumed only to touch the apices, both GDD_S and TOD_S are negative (Fig. 2b). Their sign become positive typically at $2\% < R < 6\%$ and, apart from a very few special cases, the GDD changes sign first. In the case of intracavity dispersion control, when mainly the dispersion of the laser crystal is to be compensated, it has a consequence that the prism pair operates at an R that provides full compensation for GDD and the least residual negative TOD [32]. For very short laser pulses the effect of TOD becomes significant not only on the satellite peaks but also on the pulse length [34, 35]. Here the best alignment of R is that at which the pulse length is minimal, that is where the net GDD is not zero (see e.g. [36]). In either way, once an R has been chosen, there is no more degree of freedom for changing the ratio of GDD to TOD.

Hence, at a given prism (material and apex angle) and an angle of incidence, all higher-order specific dispersion of a prism pair depends linearly only on the easily measurable R. Please note that the operation of a prism compressor based on the concept of specific values and the ratio of total glass path and prism apex distance, which has never been introduced before, can be easily and simply described.

2.2 *2.2 Temperature tuning*

By varying the temperature of the general environment of the prism pair, the phase shift at a given wavelength will change due to (i) the thermal expansion coefficient of the metal parts (optical bench, mounts, etc.), (ii) the thermal expansion coefficient and (iii) the thermal refractive index of the prism material. The first two would result in the change of R only, which is equal to setting one of the prisms to another position. Hence, no change in the GDD/TOD ratio can be expected. The point (iii) means, however, that the refractive index practically depends not only on the wavelength but also on the temperature T, that is $n = n(\lambda, T)$. Thus, the angles of refraction (3) as well as the phase shift (4) and its higher-order derivatives ((6) and (7)) will depend on the temperature.

The thermally varying values can be best characterised by calculating their derivatives with respect to T. The thermal GDD_S and TOD_S depend on temperature as

$$\mathrm{GDD_{ST}} = \frac{\partial \mathrm{GDD_S}}{\partial T} = \mathrm{GDD_{ST}} \times \left[\frac{\mathrm{d}n}{\mathrm{d}T}\left(\frac{\mathrm{d}n}{\mathrm{d}\lambda}\right)^2, \frac{\mathrm{d}n}{\mathrm{d}T}\frac{\mathrm{d}^2n}{\mathrm{d}\lambda^2}, \frac{\mathrm{d}n}{\mathrm{d}\lambda}\frac{\mathrm{d}^2n}{\mathrm{d}T\mathrm{d}\lambda}, \frac{\mathrm{d}^3n}{\mathrm{d}T\mathrm{d}\lambda^2} \right] \tag{8}$$

and

$$\mathrm{TOD_{ST}} = \frac{\partial \mathrm{TOD_S}}{\partial T} = \mathrm{TOD_{ST}} \left[\left(\frac{\mathrm{d}^2n}{\mathrm{d}T\mathrm{d}\lambda}\right)^2, \left(\frac{\mathrm{d}n}{\mathrm{d}T}\frac{\mathrm{d}n}{\mathrm{d}\lambda}\right)^2, \frac{\mathrm{d}n}{\mathrm{d}T}\left(\frac{\mathrm{d}n}{\mathrm{d}\lambda}\right)^2, \frac{\mathrm{d}n}{\mathrm{d}T}\frac{\mathrm{d}^2n}{\mathrm{d}\lambda^2}, \frac{\mathrm{d}n}{\mathrm{d}\lambda}\frac{\mathrm{d}^2n}{\mathrm{d}T\mathrm{d}\lambda}, \frac{\mathrm{d}^3n}{\mathrm{d}T\mathrm{d}\lambda^2}, \ldots \right]. \tag{9}$$

As can be seen, GDD_{ST} and TOD_{ST} are built up from the products of different orders of the derivatives of $n = n(\lambda, T)$. Hence, at a given R the ratio of the resulting group-delay dispersion and the third-order dispersion is required to vary with temperature. Moreover, a prism pair made of highly dispersive material (i.e. large $\mathrm{d}n/d\lambda$, etc.) is expected to be more sensitive to thermal changes.

3 Results

The values of specific thermal GDD and specific thermal TOD have been calculated at 800 nm for Brewster-angle prism compressors made of several optical materials as a function of the ratio of total glass path and prism apex distance. Among them three have been displayed as good examples (Fig. 3): fused silica and SF10 have positive $\mathrm{d}n/\mathrm{d}T$ and represent materials with low and high dispersion, respectively, while FK54 is one of the rare examples of optical glasses with negative $\mathrm{d}n/\mathrm{d}T$. For the glass materials the function $n = n(\lambda, T)$ was taken from the Schott catalogue [37], while the $\mathrm{d}n/\mathrm{d}T$ values for fused silica were derived from [38, 39]. From the figures it can be established that (i) the GDD_S changes less with temperature than the specific TOD_S compared to their absolute values (see also Fig. 2), (ii) the sign of the specific dispersions at $R = 0$ is the opposite to the sign of $\mathrm{d}n/\mathrm{d}T$ and (iii) for materials with large dispersion both GDD_{ST} and TOD_{ST} vary more rapidly and change sign at different $R (<\approx 25\%)$.

Figure 4 shows the typical spectral dependence of the specific thermal dispersions (group delay (GD), GDD and TOD) for two prism compressors of practical importance. The one made of a Brewster-angle fused-silica prism is to compensate the intracavity dispersion of a 2-mm-long Ti:sapphire crystal only at $R = 2.10\%$ and $l_p = 200$ mm. The other prism compressor of SF10 compensates for the extracavity dispersion of an output coupler (6.35-mm BK7) and

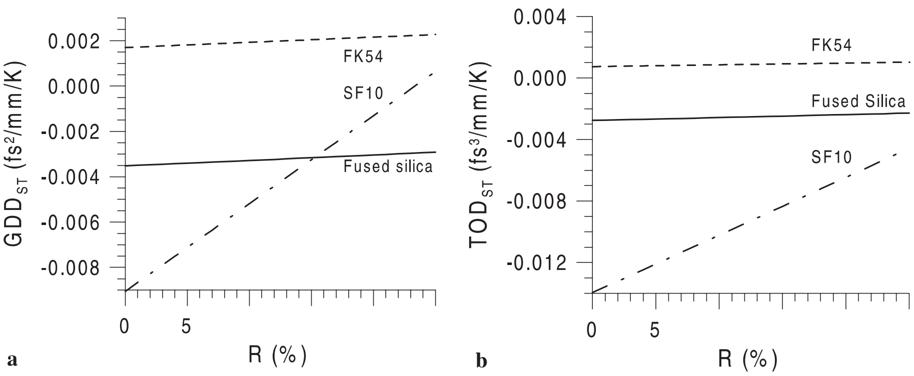

FIGURE 3 Specific thermal group-delay dispersion (GDD_{ST}) (**a**) and third-order dispersion (TOD_{ST}) (**b**) vs. ratio of total glass path and prism apex distance at 800 nm

other optics having a length of 5-mm fused silica in total. This is accomplished at $R = 4.43\%$ and $l_p = 1500$ mm. It may be worth noting that GDD_{ST} and even TOD_{ST} vary much more rapidly for SF10 than for fused silica. The strong dependence of higher-order dispersion on wavelength may be an attractive feature for compensation of such sophisticated phase shifts, which are generated upon non-collinear optical parametric amplification of ultra-short pulses [24–26, 40–43].

Another interesting consequence of the calculation is that the thermal tunability of a prism compressor is much larger towards the shorter wavelengths than in the near IR (NIR) and visible. Figure 5 shows the change of specific thermal dispersions of a fused-silica prism pair for the wavelengths of 800 nm, 400 nm and 250 nm. Since the compressors are to work with real laser pulses, to make the comparison of the expected performance at the different spectral regimes easier, the values of dispersion at the spectral half-width of 10-fs Gaussian pulses with a centre wavelength of 800 nm, 400 nm and 250 nm have also been displayed (dashed curves). As can be established, the thermal dispersion at the spectral wings of a femtosecond pulse with the same temporal length can be much larger for UV pulses than for NIR ones.

4 Experimental

Owing to the lack of a suitable Ti:sapphire oscillator, a proof-of-principle experiment has been carried out using spectrally resolved white-light interferometry [44]. A Michelson interferometer, illuminated by a halogen lamp, was constructed from optical elements having zero GDD, that is gold mirrors (M1, M2) and an achromatic beam splitter (B/S) (Fig. 6). A pair of $\varphi = 57$ °C fused-silica prisms at minimal deviation angle was placed in one arm of the Michelson interferometer and the length of the other arm was aligned to obtain white-light interference fringes. Resolving spectrally these fringes, the dispersion can be precisely established at least to the third order [44, 45] by using at least a third-order polynomial for fitting of the resulting phase shift ϕ. In order to enhance the precision of the measurement, the compressor was set to exhibit near-zero GDD at 800 nm by aligning the prisms to a prism apex distance of $l_p = 1155$ mm. The prisms were mounted on two large Peltier elements, the temperatures of which were precisely controlled and monitored.

The spectrally resolved white-light fringes were recorded at several temperatures between 22 °C and 67 °C. The measurement was repeated twice at the same temperatures both in the heating and cooling cycles. All images have been evaluated to determine GDD and TOD in the 650–900-nm spectral range. Figure 7 shows the average of the measurements along with the predicted curves. It can be seen that at 800 nm the measured thermal GDD of –3.38 fs^2/K is very close to the predicted –3.40 fs^2/K. The somewhat larger constant shift in the values of thermal TOD ($-2.16\,fs^3/K$ and –2.65 fs^3/K, respectively) is a result of the slight difference between the slopes of the measured and theoretical GDD curves. Please note that these discrepancies are still within the precision of the measurement of $\pm 0.14\,fs^2/K$ and $\pm 0.60\,fs^3/K$, respectively. The accuracy of the measurement is eventually limited by the poorer visibility of the fringes at the wings of the spectrum (see the fringes in Fig. 6), which causes larger uncertainty in the fitting parameters of the phase shift.

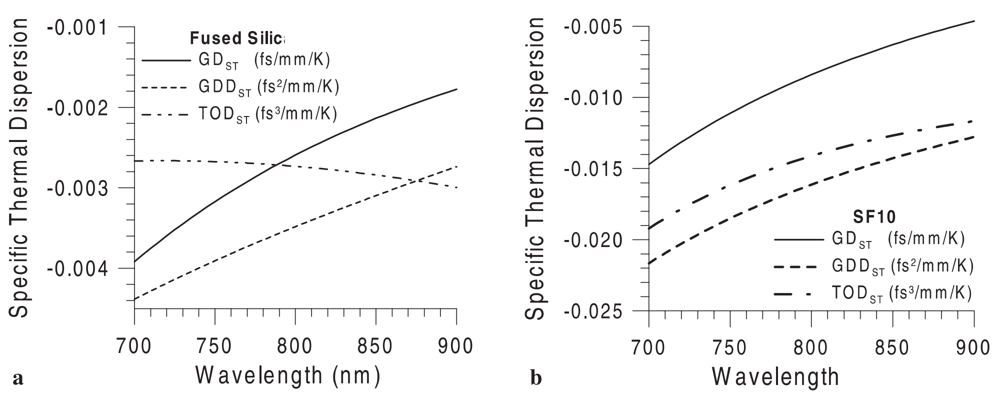

FIGURE 4 Spectral change of specific thermal dispersion for prism compressors made of fused silica (**a**) and SF10 (**b**)

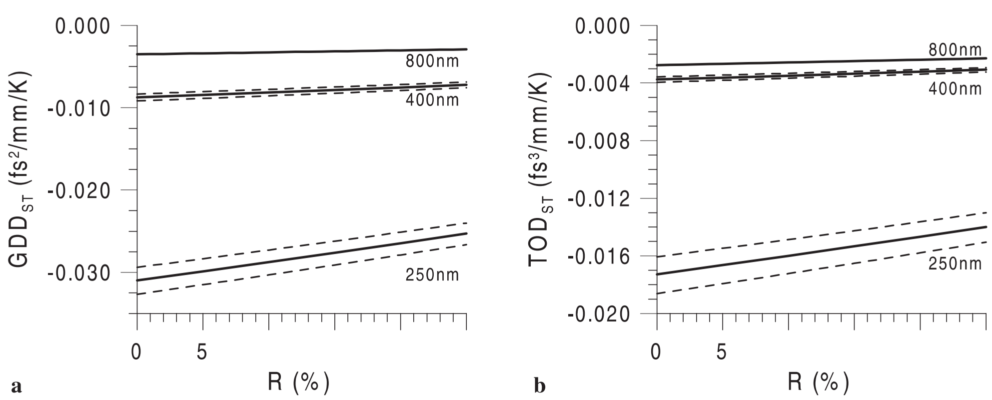

FIGURE 5 GDD_{ST} (**a**) and TOD_{ST} (**b**) of a fused-silica prism compressor for three wavelengths (*solid lines*). The *dashed lines* represent the appropriate values at the half-maxima of the spectra of 10-fs Gaussian pulses

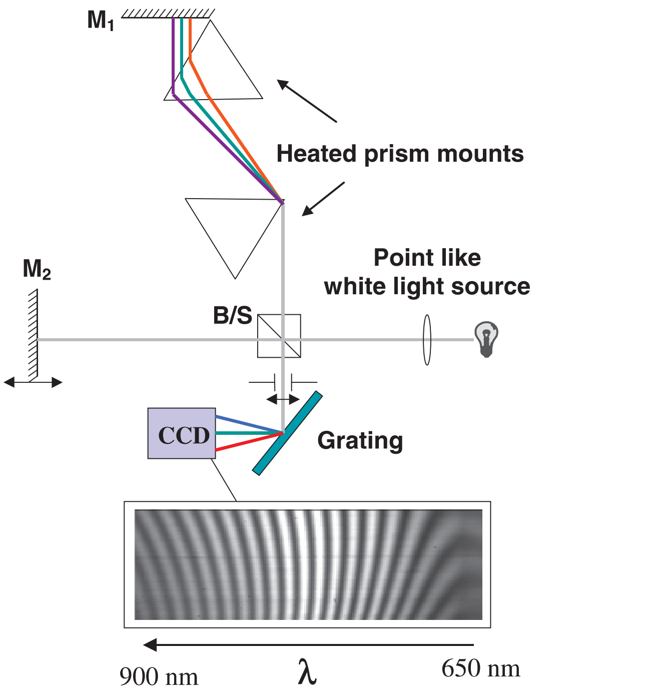

FIGURE 6 Experimental setup for measuring thermal change of the phase shift of a fused-silica prism compressor

5 Discussion

In practical applications the temperature of the prisms should be chosen very carefully. On the one hand the prism should not be cooler than the environment by 5–7 °C, otherwise water-vapour condensation would start. On the other hand if the prisms are 30–35 °C warmer than the laboratory air, both the air turbulence near the prisms and the thermal gradient of the refractive index of air can deteriorate the beam quality. These conditions allow one to calculate a maximum temperature difference of 40 °C. Please note, however, that the use of a relatively simple thin-window, low-pressure ($\approx$ 1 Torr) chamber around the prisms would almost completely stop these effects allowing a temperature difference even of 150 °C.

The higher-order dispersion control would happen in basically two ways: either the temperature of an existing intracavity prism pair is changed resulting in a 20%–30% improvement of the ratio of GDD and TOD, especially around the R values where GDD_S and TOD_S are near zero, or a second thermal prismatic compressor can be constructed. The latter case is more complicated but allows for an even more flexible adjustment.

One more rather practical consequence emerges from this study. The tight tolerance requirement of femtosecond oscillators to the higher-order dispersions as well as the sensitivity of synchronously pumped cavities to the round-trip time set a temperature-conditioning requirement for the laboratory of ± 1 °C, which corresponds to the everyday laboratory practice and was proved experimentally [46].

6 Conclusion

A practically more useful description of the operation of a prismatic pulse compressor was given by introducing the term specific dispersion, that is group-delay dispersion and third-order dispersion per unit prism apex distance. It has been shown that both GDD_S and TOD_S are linearly proportional to the ratio of the total glass path in the prisms and the prism apex distance. The temperature dependence of the refractive index of the prism material provides a new – and probably the only – extra parameter of a prismatic compressor, which makes GDD_S and TOD_S scale differently. Using temperature tuning at a given prism geometry, the accuracy of adjustment of GDD_S and TOD_S can be in the order of 0.001 fs^2/mm and 0.01 fs^3/mm, respectively. This may be necessary at generation of attosecond pulses [47] and could be successfully used also for achieving very precise locking of spectral phases of coherent pulses from two independent short-pulse oscillators [48].

ACKNOWLEDGEMENTS This work was supported by OTKA Nos. T33018 and TS040759 and FKFP No. 0170/2001. The authors are indebted to I. Ferincz, G. Kurdi and J. Klebniczki for valuable discussions.

REFERENCES

1 R.L. Fork, C.H. Bito Cruz, P.C. Becker, C-V. Shank: Opt. Lett. **12**, 483 (1987)
2 D.E. Spence, P.N. Kean, W. Sibbett: Opt. Lett. **16**, 42 (1991)
3 B.E. Lemoff, C.P.J. Barty: Opt. Lett. **18**, 57 (1993)
4 B. Proctor, F. Wise: Opt. Lett. **17**, 1295 (1992)
5 A. Müller: 'Amplification of Ultrashort Light Pulses to a Terawatt Peak Power Level at High Repetition Rate', PhD thesis, Vienna University of Technology, 2002

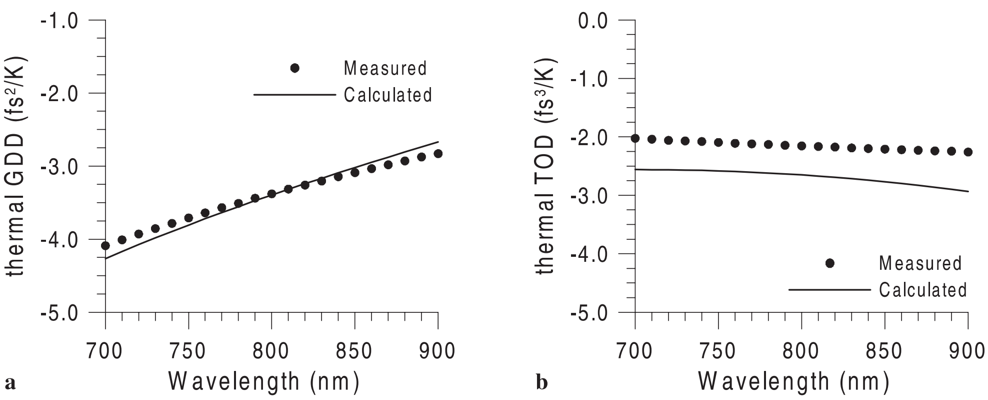

FIGURE 7 Measured and calculated spectral dependence of thermal GDD (**a**) and TOD (**b**) for a prism compressor with $l_p = 1.155$ m

6 A. Stingl, M. Lenzner, Ch. Spielmann, F. Krausz, R. Szipöcs: Opt. Lett. **20**, 602 (1995)
7 A. Baltuska, Z. Wei, R. Szipöcs, M.S. Pshenichnikov, D.A. Wiersma: Appl. Phys. B **65**, 175 (1997)
8 M. Nisoli, S. Stagira, S. DeSilvestri, O. Svelto, S. Sartania, Z. Cheng, M. Lenzner, Ch. Spielman, F. Krausz: Appl. Phys. B **65**, 189 (1997)
9 U. Morgner, F.X. Kärtner, S.H. Cho, Y. Chen, H.A. Haus, J.G. Fujimoto, E.P. Ippen, V. Scheuer, G. Angelow, T. Tschudi: Opt. Lett. **24**, 411 (1999)
10 D.H. Sutter, L. Gallmann, N. Matuschek, F. Morier-Genoud, V. Scheuer, G. Angelow, T. Tschudi, G. Steinmeyer, U. Keller: Appl. Phys. B **70**, S5 (2000)
11 J.Y. Zhou, C.J. Zhu, J. Kuhl: Appl. Phys. B **73**, 119 (2001)
12 Z. Cheng, F. Krausz, Ch. Spielmann: Opt. Commun. **201**, 145 (2002)
13 R. Szipöcs, A. Köházi-Kis: Appl. Phys. B **65**, 115 (1997)
14 N. Matuschek, F.X. Kärtner, U. Keller: IEEE J. Sel. Top. Quantum Electron. **4**, 197 (1998)
15 I. Walmsley, L. Waxer, C. Dorrer: Rev. Sci. Instrum. **72**, 1 (2001)
16 R. Szipöcs: 'Ultrafast dielectric mirror coatings': Rev. Sci. Instrum. (2002) accepted
17 A.M. Weiner: Rev. Sci. Instrum. **71**, 1929 (2000)
18 E. Zeek, K. Maginnis, S. Backus, U. Russek, M. Murnane, G. Mourou, H. Kapteyn, G. Vdovin: Opt. Lett. **24**, 493 (1999)
19 F. Verluise, V. Laude, Z. Cheng, Ch. Spielmann, P. Tournois: Opt. Lett. **25**, 575 (2000)
20 K. Osvay, K. Varjú, A.P. Kovács, G. Kurdi: 'Higher Order Dispersion Control in CPA Lasers'. In: Conf. Lasers Electro-Opt., Baltimore, USA, 2001, paper CTuM10
21 K. Osvay, M. Csatári, A. Gaál, I.N. Ross: J. Chin. Chem. Soc. **47**, 855 (2000)
22 O. Dühr, E.T.J. Nibbering, G. Korn, G. Tempea, F. Krausz: Opt. Lett. **24**, 34 (1999)
23 L. Gallmann, G. Steinmeyer, U. Keller, G. Imeshev, M.M. Fejer, J.-P. Meyn: Opt. Lett. **26**, 614 (2001)
24 G. Cerullo, M. Nisoli, S. Stagira, S. De Silvestri: Opt. Lett. **23**, 1283 (1998)
25 A. Kummrow, M. Wittmann, F. Tschirschwitz, G. Korn, E.T.J. Nibbering: Appl. Phys. B **71**, 885 (2000)
26 K. Osvay, G. Kurdi, J. Klebniczki, M. Csatári, I.N. Ross: Appl. Phys. Lett. **80**, 1704 (2002)
27 O.E. Martinez, J.P. Gordon, R.L. Fork: J. Opt. Soc. Am. A **1**, 1003 (1984)
28 R.L. Fork, O.E. Martinez, J.P. Gordon: Opt. Lett. **9**, 150 (1984)
29 Z. Bor, K. Osvay, H.A. Hazim, A. Kovács, G. Szabó, B. Rácz, O.E. Martinez: Opt. Commun. **90**, 70 (1992)
30 V. Petrov, F. Noack, W. Rudolph, C. Rempel: Exp. Techn. Phys. **36**, 167 (1988)
31 Z. Bor, B. Rácz: Opt. Commun. **54**, 165 (1985)
32 R.E. Sherriff: J. Opt. Soc. Am. B **15**, 1224 (1998)
33 F.J. Duarte: Opt. Quantum Electron. **22**, 467 (1990)
34 G.P. Agrawal, M.J. Potasek: Phys. Rev. A **3**, 1765 (1986)
35 H. Wang, S. Backus, Z. Chang, R. Wagner, K. Kim, X. Wang, D. Umstadter, T. Lei, M. Murnane, H. Kapteyn: J. Opt. Soc. Am. B **16**, 1790 (1999)
36 K.C. Chan, H.F. Liu: Opt. Lett. **19**, 49 (1994)
37 Schott Group: www.schott.com
38 I.H. Malitson: Appl. Opt. **2**, 1103 (1963)
39 J. Matsuoka, N. Kitamura, S. Fujinaga, T. Kitaoka, H. Yamashita: J. Non-Cryst. Solids **135**, 86 (1991)
40 E. Riedle, M. Beutter, S. Lochbrunner, J. Piel, S. Schenkl, S. Spörlein, W. Zinth: Appl. Phys. B **71**, 457 (2000)
41 A. Shirakawa, I. Sakane, M. Takasaka, T. Kobayashi: Appl. Phys. Lett. **74**, 2268 (1999)
42 D. Zeidler, T. Hornung, D. Proch, M. Motzkus: Appl. Phys. B **70**, S125 (2000)
43 I.N. Ross, P. Matousek, G.H.C. New, K. Osvay: 'An analysis and optimisation of optical parametric chirped pulse amplification': J. Opt. Soc. Am. B **19** (2002) in print
44 A.P. Kovács, K. Osvay, Z. Bor, R. Szipöcs: Opt. Lett. **20**, 788 (1995)
45 Z. Bor, A.P. Kovács, K. Osvay, R. Szipöcs: SPIE 3359, 132 (1998)
46 V. Francois, S. Lagacé, X. Guan, S.L. Chin: Appl. Opt. **33**, 5522 (1994)
47 M. Hentschel, R. Kienberger, C. Spielmann, G.A. Reider, N. Milosevic, T. Brabec, P. Corkum, U. Heinzmann, M. Drescher, F. Krausz: Nature **414**, 509 (2001)
48 R.K. Shelton, L.-S. Ma, H.C. Kapteyn, M.M. Murnane, J.L. Hall, J. Ye: Science **293**, 1286 (2001)